Analysis of β-Casein−Monopalmitin Mixed Films at the Air−Water Interface

Juan M. Rodríguez Patino,* Cecilio Carrera Sánchez, and M. Rosario Rodríguez Niño

Departamento de Ingeniería Química, Facultad de Química, Universidad de Sevilla, c/Profesor García González s/núm, 41012 Seville, Spain

The surface pressure (π)−area (A) isotherms and Brewster angle microscopy (BAM) images of monopalmitin and β-casein mixed films spread on buffered water at pHs 5 and 7 and at 20 °C were determined as a function of the mass fraction of monopalmitin in the mixture (X). The structural characteristics and morphology of monopalmitin−β-casein mixed films are dependent on surface pressure, pH, and monolayer composition. The prevalence of monopalmitin in the interface increases with the amount of monopalmitin in the mixture and at higher π. At the monopalmitin monolayer collapse the mixed film is practically dominated by the presence of monopalmitin. However, some degree of interactions exist between monopalmitin and β-casein in the mixed film, and these interactions are more pronounced as the monolayer is compressed at the highest surface pressures.

Keywords: *Monopalmitin; β-casein; food emulsifier; mixed film; air−water interface*

INTRODUCTION

Food emulsions cover an extremely wide area in practical applications—including products that contain both solids and gases in addition to two liquid phases (i.e., ice cream)—although these dispersed systems are inherently unstable from a thermodynamic and kinetic point of view. From a practical point of view, food emulsions need to be stable because many of them are designed to have a long shelf life. The stability of food emulsions is complex because it covers both a number of phenomena and a variety of systems with different contents (Dickinson, 1992; Friberg and Larsson, 1997; Sjöblom, 1996). Oil-in-water emulsions (i.e., ice cream, cream liqueurs, mayonnaise, etc.) are stabilized by the adsorption of small-molecular-weight emulsifiers (i.e., polar lipids, such as mono- and diglycerides), protein molecules (milk and egg proteins), or aggregates of protein molecules (i.e., casein micelles) or by a mixture of these (Bos et al., 1997). However, water-in-oil emulsions (i.e., spreads, margarine, butter, etc.) are mainly stabilized by mechanical actions (i.e., high bulk-phase viscosity, adsorption of liquid crystals at the interface, oil crystallization, etc.) (Dalgleish, 1996).

Proteins and polar lipids typically coexist in food emulsions, sometimes unassociated with each other but also in association, with specific actions in the processing and properties of the final product. Polar lipids adsorb strongly to fluid−fluid interfaces, giving close molecular packing at the interface, which produces low surface and interfacial tensions (Rodríguez Niño and Rodríguez Patino, 1998a,b). However, they do not produce highly cohesive or viscous layers (especially at the oil−water interface). Proteins, on the other hand, act as polymeric emulsifiers with multiple anchoring sites at the interface that, together with the unfolding process of the protein molecule when adsorbed at the interface (Rodríguez Niño et al., 1997a,b; Rodríguez Patino et al., 1999a), stabilizes the interfacial layer kinetically. Proteins and lipids have an important physical property in common, their amphiphilic nature. This property provides the possibility for association, adsorption, and reorientation at fluid−fluid interfaces, depending on the properties of the components and the protein−lipid ratio (Rodríguez Niño and Rodríguez Patino, 1998a,b; Rodríguez Niño et al., 1998a,b). The competitive adsorption and/or displacement between lipids and proteins at fluid−fluid interfaces have been studied in detail in several investigations. For further information concerning the interfacial characteristics of food emulsifiers (proteins and lipids), the reader is referred to recent reviews (Bos et al., 1997; Damodaran and Paraf, 1997; Friberg and Larsson, 1997; Nylander and Ericsson, 1997; Sjöblom, 1996; Cayot and Lorient, 1997; Dalgleish, 1996, 1997). However, so far, little is know about the structure that proteins and lipids adopt at fluid−fluid interfaces.

In this paper we present an extension of previous studies on the application of the film balance and a recent noninvasive technique, Brewster angle microscopy (BAM), to analyze the morphological characteristics of β-casein and monopalmitin mixed films at the air−water interface. The film balance makes it possible to analyze the structural characteristics (Rodríguez Patino et al., 1992 and 1993) by means of the surface-pressure−area isotherm (π−A isotherm). The BAM technique allows visualization of the structure that heterogeneous domains form at the air−water interface (Rodríguez Patino et al., 1999b,c,d). In addition, by BAM measurement of the relative reflectivity (I) and relative film thickness (δ) are also possible if a model is adopted for molecular domains at the interface or by calibration of the light in the camera (de Mul and Mann, 1998; Rodríguez Patino et al., 1999b,c,d). In this paper we have demonstrated that BAM is a useful tool for the analysis of protein−lipid mixed films at the air−water interface.

* To whom correspondence should be addressed (telephone +34 95 4557133; fax +34 95 4557134, e-mail jmrodri@cica.es).

10.1021/jf9902696 CCC: $18.00
Published on Web 11/12/1999

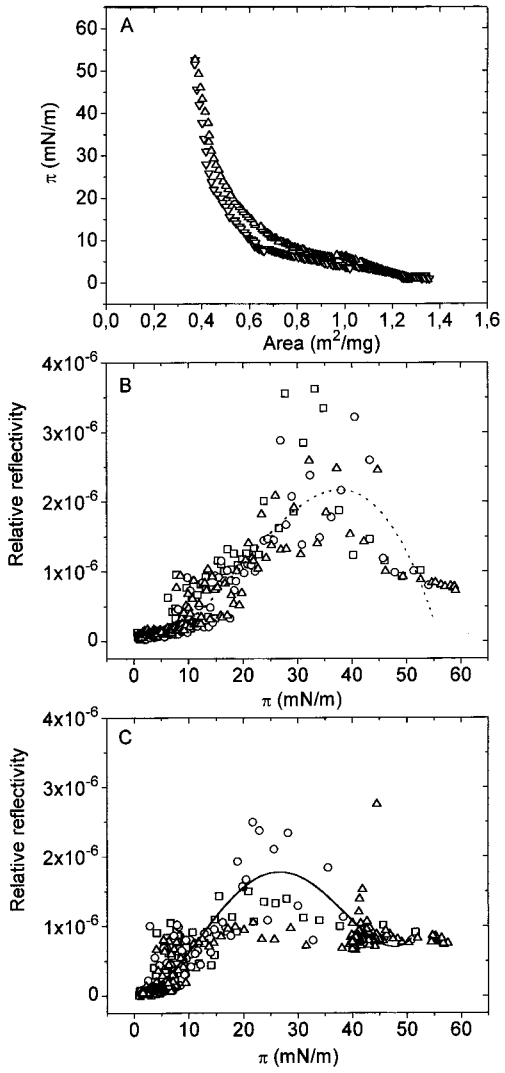

Figure 1. (A) $\pi-A$ isotherm for monopalmitin monolayer during a compression (Δ) and expansion (∇) cycle. (B and C) Relative reflectivity as a function of surface pressure during the compression and expansion, respectively, for monopalmitin monolayers (different symbols are for different experiments) at a shutter speed of 1:250 s. Aqueous-phase pH = 7. Temperature 20 °C. The lines fit the experimental $I-\pi$ data (10 measurements) by means of a fourth-order polynomial.

MATERIALS AND METHODS

Chemicals. Danisco Ingredients (Denmark) supplied synthetic 1-monohexadecanoyl-*rac*-glycerol (monopalmitin) with over 95−98% purity. To form the surface film, monoglyceride was spread in the form of a solution using hexane:ethanol (9:1, v:v) as a spreading solvent. Analytical-grade hexane (Merck (Darmstadt, Germany), 99%) and ethanol (Merck, >99.8%) were used without further purification. β-Casein (99% pure) was supplied and purified from bulk milk from the Hannah Research Institute, Ayr, Scotland (Atkinson et al., 1995, 1997). Samples for interfacial characteristics of β-casein films were prepared using Milli-Q (Milford, MA) ultrapure water and buffered at pH 7. Analytical-grade acetic acid, sodium acetate, and Trizma, [tris(hydroxymethyl)aminomethane], for buffered solutions were used as supplied by Sigma (St. Louis, MO, >95%) without further purification. Ionic strength was 0.05 M in all the experiments. The absence of active surface contaminants in the aqueous buffered solutions was checked by surface tension measurements before sample preparation. No aqueous solutions with a surface tension other than that accepted in the literature (72−73 mN/m at 20 °C) were used.

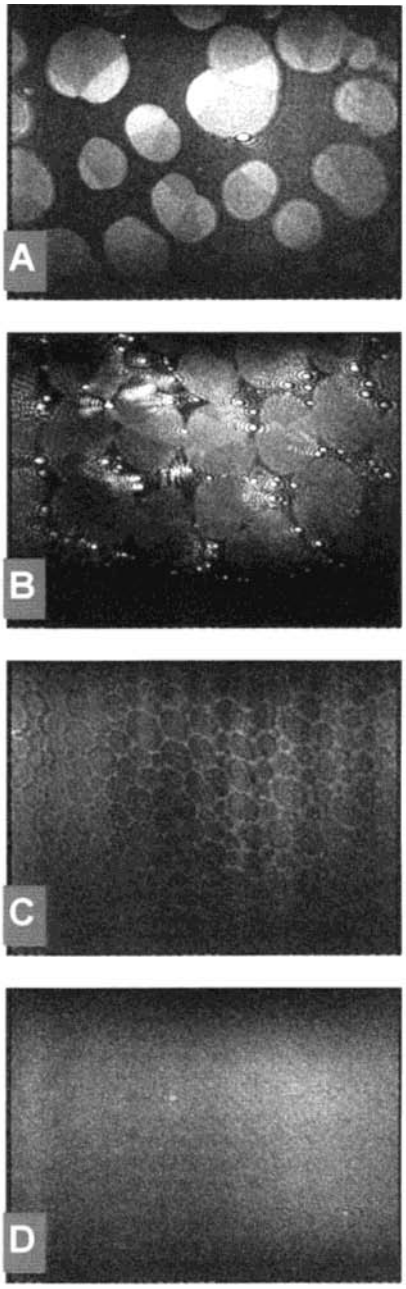

Figure 2. Visualization of (A, B, and C) monopalmitin and (D) β-casein pure monolayers by Brewster angle microscopy at 20 °C and at pH 7. (A) monopalmitin monolayer at $\pi = 10$ mN/m, (B) monopalmitin monolayer at $\pi = 35$ mN/m, (C) 2D foam after expansion of monopalmitin monolayer at $\pi = 4$ mN/m, and (D) β-casein monolayer at $\pi = 20$ mN/m. The horizontal direction of the image corresponds to 630 μm and the vertical direction to 470 μm.

Surface Film Balance. Measurements of the surface pressure (π) versus average area per molecule (A) were performed on a fully automated Langmuir-type film balance using a maximum area of 5.62×10^{-2} m^2, as described elsewhere (Rodríguez Patino et al., 1992, 1993). The mean deviation was within ±0.1 mN/m for surface pressure and $\pm 0.125 \times 10^{-3}$ m^2/mg for area. The subphase temperature was controlled at 20 °C by water circulation from a thermostat, within an error range of ±0.5 °C. The temperature was measured by a thermocouple located just below the air−water interface.

Before each measurement, the film balance was calibrated at 20 °C. Mixtures of particular mass ratios—ranging between 0 and 1, expressed as the mass fraction of monopalmitin in the mixture, X—were studied. To allow the quantitative

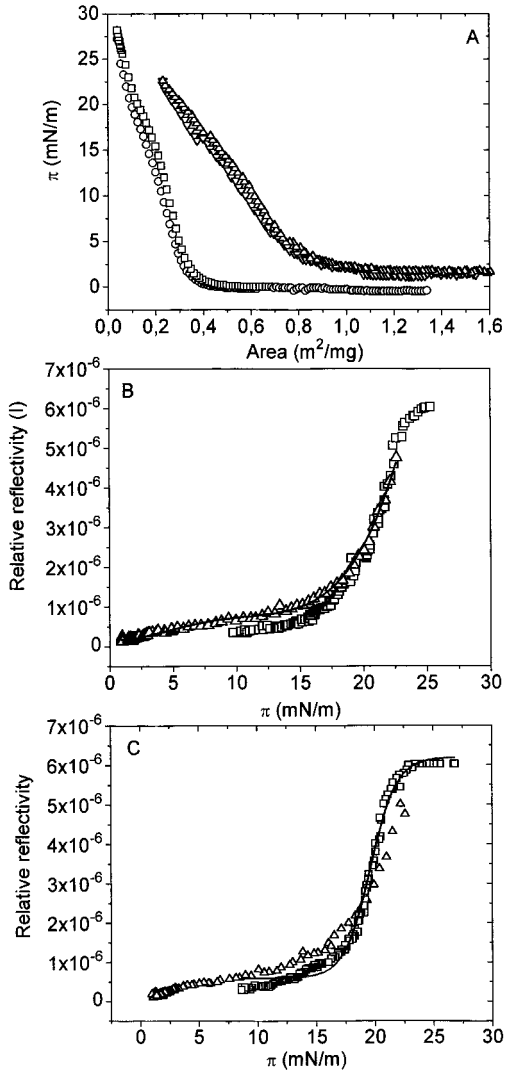

Figure 3. (A) $\pi-A$ isotherms for β-casein monolayers at pH 5 (○, □) and at pH 7 (Δ, ∇), during a compression (□, Δ)−expansion (○, ∇) cycle. (B and C) Relative reflectivity as a function of surface pressure during the compression and expansion, respectively, for β-casein monolayers at pH 5 (□) and 7 (Δ) and at a shutter speed of 1:250 s. Temperature 20 °C. The lines fit the experimental $I-\pi$ data (10 measurements) by means of a sigmoidal function.

adsorption of the protein on the interface, the monolayer was not under any surface pressure during the spreading process. Thus, the β-casein necessary to form the mixed film should be spread before the lipid. Aliquots ranging from 175 to 475 μL of aqueous solutions of β-casein (1.543×10^{-4} mg/μL) at pH 7 were spread on the interface by means of a micrometric syringe. To allow for spreading, adsorption, and rearrangements of the protein, 30 min was allowed to elapse before measurements were taken. The spreading method adopted in these experiments ensured quantitative spreading of the protein on the interface as discussed in a previous paper (Rodríguez Niño et al., 1998c). Afterward, monopalmitin solutions in a hexane:ethanol mixture were spread at different points on the β-casein film. To allow for spreading and β-casein−monopalmitin interactions, 30 min was allowed to elapse before compression was performed. To ensure interactions and homogeneity, the mixed film was compressed near the collapse point of the mixture and then expanded immediately to avoid the collapse. After 30 min at the maximum area, measurements of compression−expansion cycles were performed with 30 min of waiting time between each expansion−compression cycle. The compression rate was 3.3 cm·min^{-1}, which is the highest value for which isotherms have been found to be reproducible in preliminary experiments. Each isotherm

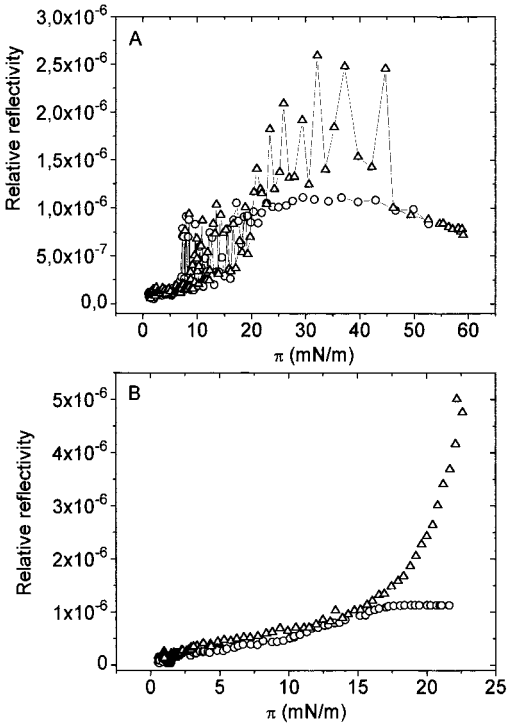

Figure 4. Relative reflectivity as a function of surface pressure for (A) monopalmitin and (B) β-casein spread monolayers at the air−water interface at 20 °C and at pH 7 for a shutter speed of (○) 1:50 and (Δ) 1:250 s.

was measured at least 4 times. The reproducibility of the surface pressure results were better than ±0.5 mN/m. All isotherms were recorded continuously by a device connected to the film balance and then analyzed off-line.

Brewster Angle Microscope (BAM). A commercial Brewster angle microscope (BAM), BAM2, manufactured by NFT (Göttingen, Germany) was used to study the morphology of the monolayer. Further characteristics of the device and operational conditions were described elsewhere (Rodríguez Patino et al., 1999b,c). The BAM was positioned over the film balance on a specially designed frame structure that makes it easy to move the BAM along the length of the film balance. The location of the BAM along the film balance makes it possible to visualize any inhomogeneity in the overall film. The surface pressure measurements, area, and gray level as a function of time were carried out simultaneously by means of a device connected between the film balance and the BAM. The frequency was fixed at one measurement every 5 s in order to reduce the noise in the gray level signal not related to the optical properties of the monolayer. These measurements were performed during continuous compression and expansion of the monolayer at a constant rate with different shutter speeds (integration time) ranging from 1:50 to 1:500 s. The camera shutter timing makes it possible to select the exposure time to adapt to different illumination levels.

To measure the relative thickness of the film, a camera calibration is necessary previously in order to determine the relationship between the gray level (GL) and the relative reflectivity (I), according to a procedure described previously (Rodríguez Patino et al, 1999b,c). The intensity at each point in the BAM image depends on the local thickness and film optical properties. These parameters can be measured by determining the light intensity at the camera and analyzing the polarization state of the reflected light through the method based on the Fresnel reflection equations (Azzam and Bashara, 1992). At the Brewster angle

$$I = |R_p|^2 = C\delta^2 \qquad (1)$$

where I is the relative reflectivity ($I = I_o/I_r$, where I_r and I_o

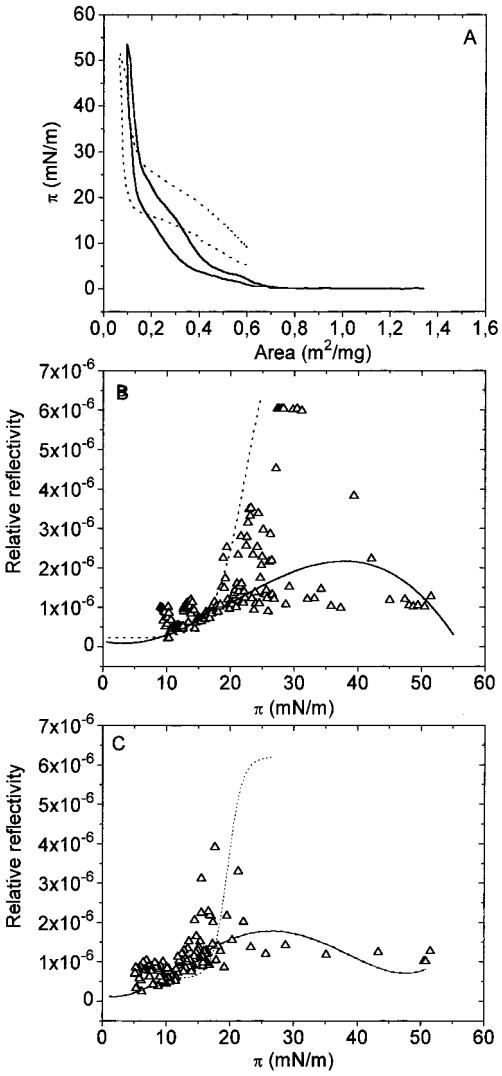

Figure 5. (A) $\pi-A$ Isotherms for monopalmitin−β-casein mixed monolayers at pH 5 (—) and pH 7 (···). (B and C) Relative reflectivity as a function of surface pressure during the compression and expansion, respectively, for monopalmitin−β-casein monolayers at pH 7 (Δ) and at a shutter speed of 1:250 s. Temperature 20 °C. Monopalmitin mass fraction in the mixture: $X = 0.2$. The line fit for monopalmitin (—) and β-casein (···) pure monolayers are included in plots B and C.

are the reflected intensity and the incident intensity, respectively), C is a constant, δ is the film thickness, and R_p is the p-component of the light.

RESULTS AND DISCUSSION

Single Monolayer Components. *Monopalmitin.* Figure 1 shows the $\pi-A$ isotherm (Figure 1A) and the relative reflectivity versus surface pressure for compression (Figure 1B) and expansion (Figure 1C) of a monopalmitin monolayer at 20 °C and pH 7. Similar results were observed for a monopalmitin monolayer at 20 °C and pH 5 (data not shown). The evolution with the surface pressure of the relative reflectivity of BAM images (Figure 1B,C) gives complementary information on the structural characteristics of spread monopalmitin monolayers deduced from the $\pi-A$ isotherm (Figure 1A). Monopalmitin monolayer adopts different structures (Figure 1A) with different morphologies, as visualized by BAM (Figure 2) as a function of surface pressure. A liquid-expanded structure with a homogeneous morphology was observed at $\pi < 5$ mN/m. In this region the $I-\pi$ plot is a continuous line without any significant noise (Figure 1B). A degenerate first-order phase transition between liquid-expanded and liquid-condensed structures, with circular liquid-condensed domains in a homogeneous liquid-expanded ambient (Figure 2A), was observed at $5 < \pi < 30$ mN/m. The existence of noise peaks in the $I-\pi$ plot (Figure 1B) was observed when a circular liquid-condensed domain passed through the spot where this measurement was performed. This phenomenon denotes morphological film anisotropy and differences in film thickness at a microscopic scale. The liquid-condensed structure was observed at $\pi > 30$ N/m, with circular and anisotropic domains which grow with surface pressure (Figure 2B). In this region the noise peaks increased in intensity. Finally, the collapse phase was observed at a surface pressure of about 53.1 mN/m, characterized by a homogeneous morphology after fusion of liquid-condensed circular domains. The noise peak vanished and the relative intensity decreased at higher surface pressures as the monolayer collapsed (Figure 1B). After expansion, monopalmitin monolayer undergoes break up of the collapsed structure to a 2D foam structure (Figure 2C). The noise peaks were of lower intensity, and the relative intensity was lower during monolayer expansion, especially for the liquid-condensed structure at $\pi > 25$ mN/m (Figure 1C). In summary, the domains in BAM images and peaks in $I-\pi$ plots (Figure 1) reflect the distribution of monopalmitin molecules, the packing density, and the film thickness (in accordance with eq 1) as a function of the surface pressure and the compression−expansion direction.

β-Casein. Figure 3 shows the $\pi-A$ isotherm (Figure 3A) and the relative reflectivity versus surface pressure, $I-\pi$, plot for compression (Figure 3B) and expansion (Figure 3C) of β-casein monolayers at 20 °C and pHs 5 and 7. It can be seen that β-casein monolayers have a liquid-expanded-like structure under these experimental conditions, but the $\pi-A$ isotherm was displaced toward the π axis, and the monolayer structure is more condensed in acidic subphase (Figure 3A). At a surface pressure of ca. 25 mN/m, the β-casein monolayer collapses. These results were reproducible within the experimental error as were those obtained with the same protein by application of several available methods for protein spreading (Rodríguez Niño et al., 1998c). The $I-\pi$ plots reflect the surface equation of state for β-casein spread monolayers. As for the $\pi-A$ isotherm (Figure 3A), the $I-\pi$ curve was displaced toward the I axis during expansion (Figure 3C), indicating that the molecular reorganization of β-casein at the interface upon expansion requires some time, as a consequence of its viscoelastic characteristics. The relative reflectivity increased with the monolayer compression and tended to plateau at the collapse point, but neither first-order transition nor crystalline domains were observed as for monopalmitin (Figure 1). The absence of any ordered structures reduced the noise peak in the $I-\pi$ plot either under monolayer compression or expansion, a consequence of the monolayer isotropy as deduced from BAM images (Figure 2D). It should be emphasized that β-casein monolayers saturate the camera (image completely white) after the collapse point for surface pressures higher than 25 mN/m, with a shutter speed of 1:250 s, a phenomenon not observed for monopalmitin monolayer.

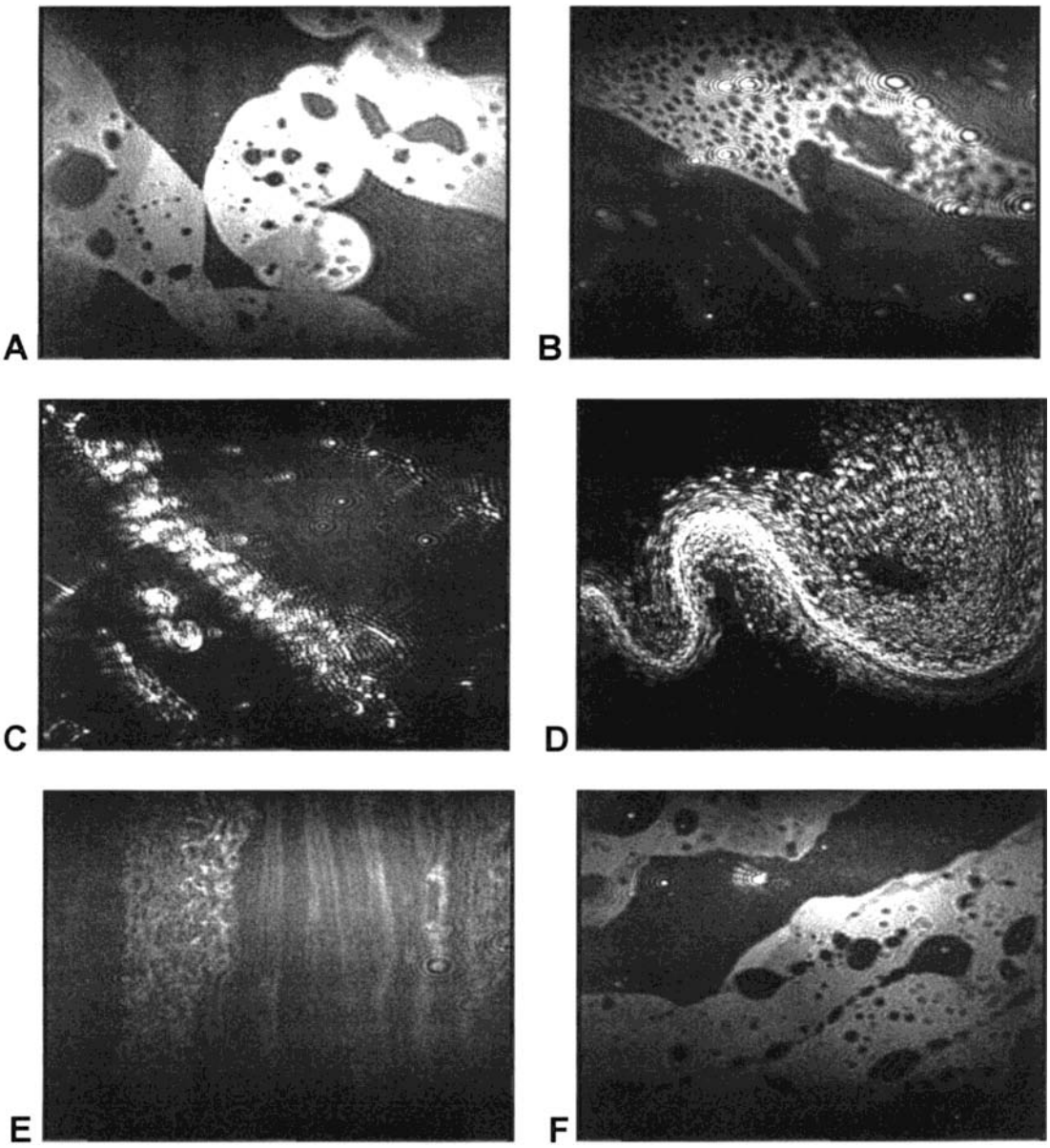

Figure 6. Visualization of monopalmitin−β-casein mixed monolayers by Brewster angle microscopy at 20 °C and pH 7 (A) π = 9 mN/m, (B) π = 25 mN/m (at the β-casein collapse), (C) π = 50 mN/m (at the monopalmitin collapse), (D) monolayer expansion at π = 25 mN/m, (E) 2D foam after monolayer expansion at π = 15 mN/m, and (F) 2D foam after monolayer expansion at π = 7 mN/m. Monopalmitin mass fraction in the mixture: $X = 0.2$. The horizontal direction of the image corresponds to 630 μm and the vertical direction to 470 μm.

Effect of the Shutter Speed. Due to the fact that the relative reflectivity is higher for protein (Figure 3) than for lipid (Figure 1) monolayers (Rodríguez Patino et al., 1999b,c), the shutter speeds must be optimized. The effect of shutter speed on relative reflectivity was determined for monopalmitin and β-casein components in the range of 1:50−1:500 s. The higher the shutter numbers, the shorter the exposure time and the greater the amount of light required to obtain an image. Figure 4 shows the $I-\pi$ plots for monopalmitin (Figure 4A) and β-casein (Figure 4B) at two representative shutter speeds, as an example. At the lower shutter speeds, the noise in the $I-\pi$ plot associated with the existence of liquid-condensed monopalmitin domains decreased. But this low shutter speed is inappropriate for the analysis of monopalmitin monolayers—in the range of existence of liquid-condensed domains (Figure 4A)—and for β-casein monolayers—at surface pressures near the collapse and, especially, at the collapse point (Figure 4B)—due to camera saturation. However, the opposite applies at higher shutter speeds. With high shutter speed values, the range for I measurements increased, which is useful for the analysis of lipids with liquid-condensed structures, but the noise in the $I-\pi$ plot increased. In addition, at the highest shutter speed (1:500 s) the camera was saturated with a thick protein film (image completely white), even after the protein collapse. From preliminary experiments (Figure 4) it was deduced that a shutter speed of 1:250 s is adequate for the analysis of β-casein−monopalmitin mixed monolayers. However, for mixed films in the range of high pressures (near and after the β-casein collapse), the relative reflectivity is high enough and saturation of the camera was observed at a shutter speed of 1:250 s. This phenomenon is due to the higher thickness of the mixed monolayer with respect to pure components, as will be discussed later.

Mixed Components. The differences observed between monopalmitin (Figure 1) and β-casein (Figure 3)

monolayers in structure, morphology (Figure 2), and relative reflectivity during the compression−expansion cycle will be used in the next section to analyze the application of BAM to β-casein−monopalmitin mixed monolayers. For comparison purposes, a continuous line was deduced by fitting the $I-\pi$ data, derived from different measurements. The use of $I-\pi$ lines for single components in the analysis of β-casein−monopalmitin mixed films is of great utility, especially for monopalmitin monolayer. As discussed above, $I-\pi$ plots for monopalmitin monolayers in the liquid-expanded to liquid-condensed transition and, especially, with a liquid-condensed structure have many peaks with different intensities. The existence of these peaks, due to the passage of an liquid-condensed domain through the measurement spot, is a random phenomenon which could be normalized by the fitting of the $I-\pi$ data derived from different measurements (10 measurements in this work) with a fourth-order polynomial. In addition, the reproducibility of the measurements for β-casein films was demonstrated by the close agreement between the parameters derived from a sigmoidal fitting (data not shown) of $I-\pi$ plots for 10 measurements with the same monolayer.

Monopalmitin−β-Casein Mixed Film at a Mass Fraction of Monopalmitin in the Mixture of 0.2. In Figure 5 we show the $\pi-A$ isotherm for a compression−expansion cycle (Figure 5A) and the $I-\pi$ plots for compression (Figure 5B) and expansion (Figure 5C) of monopalmitin−β-casein mixed monolayer at 0.2 in mass fraction of monopalmitin in the mixture. In Figure 6 we show the BAM images for mixed films at some representative surface pressures during the compression−expansion cycle.

During the monolayer compression at low surface pressures, the $I-\pi$ plot for the mixed film was essentially the same as for pure monopalmitin and β-casein monolayers (Figure 5B). A continuous line fit the data at $\pi < 5$ mN/m due to the fact that both monopalmitin and β-casein monolayers adopt an expanded structure (Figure 5A) and a homogeneous morphology. At 5 mN/m the onset, in the liquid-expanded to liquid-condensed transition was observed (Figure 5A), as for monopalmitin (Figure 1A). At $\pi > 5$ mN/m, the existence of some noise peaks was observed when liquid-condensed domains of monopalmitin in an homogeneous liquid-expanded ambient of monopalmitin, and probably of an homogeneous β-casein film as well, passed through the spot where this measurement was performed (Figure 5B). Although the liquid-condensed monopalmitin domains can be well characterized by the BAM images (Figure 6A)—i.e., by turning the analyzer from 60° to 120° (Rodríguez Patino et al., 1999b), data not shown—we are unable to distinguish between monopalmitin and β-casein domains in the continuous homogeneous phase. It should be noted that the morphology of the mixed film in this region is significantly different than that for pure components. It can be seen that the domains did not appear with a characteristic circular shape, as for monopalmitin (Figure 1B), but as a network along the image, a phenomenon that we associated with the existence of protein−lipid interactions.

At higher surface pressures (at $\pi = 20-25$ mN/m), near the β-casein collapse (Figure 3A), the intensity of the noise peaks increased and the relative intensity of some spots was the same as for pure β-casein. This is due to the fact that in this region domains of pure β-casein (with high I) and monopalmitin (with low I) passed alternatively through the spot (Figure 5B). In the region after the β-casein collapse (25−35 mN/m), the camera is saturated with high I values with a high frequency, characteristic of the β-casein monolayer at the collapse. From the BAM image (Figure 6B), the squeezing out of β-casein by monopalmitin can be distinguished, in a region with liquid-condensed domains of monopalmitin over a sublayer of collapsed protein (image completely white). Outside this region liquid-condensed domains of closely packed monopalmitin dominate the monolayer.

After the β-casein collapse and before the monopalmitin collapse (at 35 mN/m $< \pi <$ 52 mN/m), both the relative reflectivity and the noise peaks decreased to even lower values than for monopalmitin. This suggests that in this region the lipid predominates at the interface but, due to the existence of a sublayer of β-casein molecules, the lipid domains are so closely

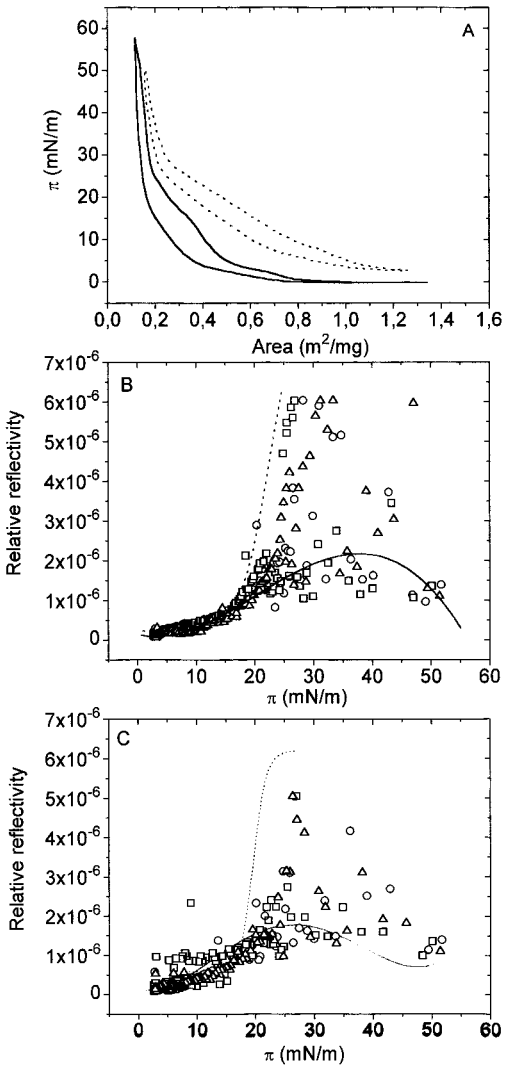

Figure 7. (A) $\pi-A$ isotherms for monopalmitin−β-casein mixed monolayers at pH 5 (—) and pH 7 (···). (B and C) Relative reflectivity as a function of surface pressure during the compression and expansion, respectively, for monopalmitin−β-casein monolayers at pH 7 (different symbols are for repetitive measurements) and at a shutter speed of 1:250 s. Temperature 20 °C. Monopalmitin mass fraction in the mixture: $X = 0.4$. The line fit for monopalmitin (—) and β-casein (···) pure monolayers are included in plots B and C.

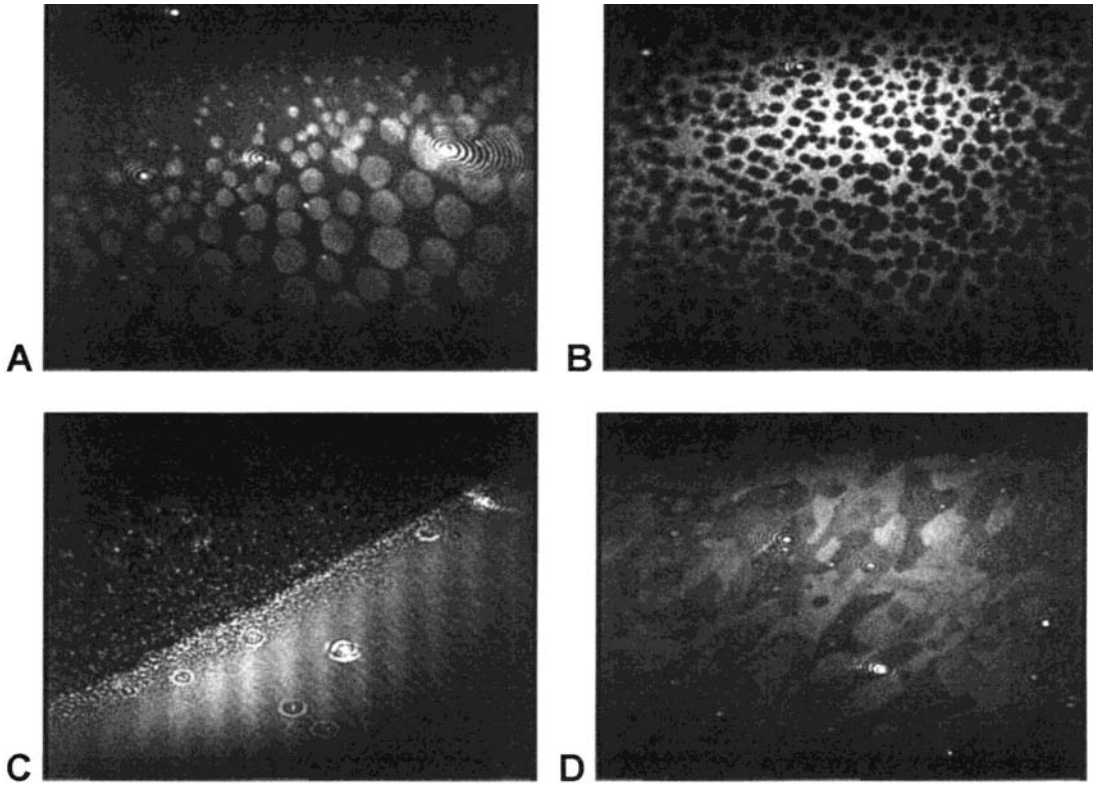

Figure 8. Visualization of monopalmitin−β-casein mixed monolayers by Brewster angle microscopy at 20 °C and pH 7. (A) π = 14 mN/m, (B) squeezing out phenomena at π = 26 mN/m (at the β-casein collapse), (C) π = 45 mN/m (near the monopalmitin collapse), and (D) 2D foam after monolayer expansion at π = 12 mN/m. Monopalmitin mass fraction in the mixture: X = 0.4. The horizontal direction of the image corresponds to 630 μm and the vertical direction to 470 μm.

packed that the monolayer morphology acquires a high homogeneity.

Finally, at the lipid collapse (at $\pi \cong$ 52 mN/m) the relative reflectivity is practically the same as that for monopalmitin. Surprisingly, in this region of highest surface pressure different paths of collapsed β-casein can be observed in a homogeneous region of collapsed monopalmitin (Figure 6C), by translation of the BAM along the length of the film balance. For the first time it has been demonstrated that the lipid is unable to displace all β-casein molecules from the interface, even at the highest surface pressure.

With the monolayer expansion this path of collapsed protein was deformed by the interfacial shear in the direction of the barrier movement, giving a thin stream of collapsed β-casein molecules to which liquid-condensed domains of monopalmitin adhered (Figure 6D). This morphology prevailed during the expansion, even at surface pressures lower than that for the β-casein collapse (Figure 6E). The overall morphology of the monolayer during the expansion at lower surface pressures is the formation of 2D foam after the break up of the collapsed structure. However, the 2D foam morphology (Figure 6F) was different from those for pure components probably due to the penetration of β-casein molecules in the monopalmitin monolayer with the expansion. We cannot reject the existence of some degree of mixing between monopalmitin and β-casein after the monolayer collapse but it is impossible to distinguish this fact from the BAM images alone. The $I-\pi$ curve during the monolayer expansion is similar to that of monopalmitin at surface pressures higher than that for β-casein collapse but is practically similar to those for single components at lower surface pressures. It should be noted that at π lower than ca. 25 mN/m, some noise peaks have a higher intensity than those for pure β-casein, a phenomenon not observed during the monolayer compression.

In summary, the results reported here suggest that in monopalmitin−β-casein mixed films, islands of protein and lipid do exist at the air−water interface on a microscopic level, depending on the surface pressure and the direction of the compression−expansion cycle.

Monopalmitin−β-Casein Mixed Film at a Mass Fraction of Monopalmitin in the Mixture of 0.4. In Figure 7 we show the $\pi-A$ isotherm for a compression−expansion cycle (Figure 7A) and the $I-\pi$ plots for compression (Figure 7B) and expansion (Figure 7C) of monopalmitin−β-casein mixed monolayer at 0.4 in mass fraction of monopalmitin in the mixture. In Figure 7B,C we only include the results of three measurements to add clarity (six $I-\pi$ plots were recorded for compression−expansion cycles with the same monolayer). In Figure 8 we show the BAM images for mixed films at some representative surface pressures during the compression−expansion cycle.

The monolayer structure in monopalmitin−β-casein mixed films (Figure 7A) at surfaces pressures lower than β-casein collapse (at $\pi \cong$ 25 mN/m) adopt a structural polymorphism, as for monopalmitin (Figures 1A). Moreover, it can be seen that there was a monolayer expansion as both the pH and the monopalmitin content in the mixture were increased (Figures 1A, 5A, and 7A). At surface pressures higher than that for β-casein collapse, the $\pi-A$ isotherms for mixed monolayers were parallel to that of monopalmitin. These results suggest that the composition of mixed monolayers was very dependent on the surface pressure (Rodríguez Patino et al., 1999d). At surface pressures lower than that for β-casein collapse, a mixed monolayer of

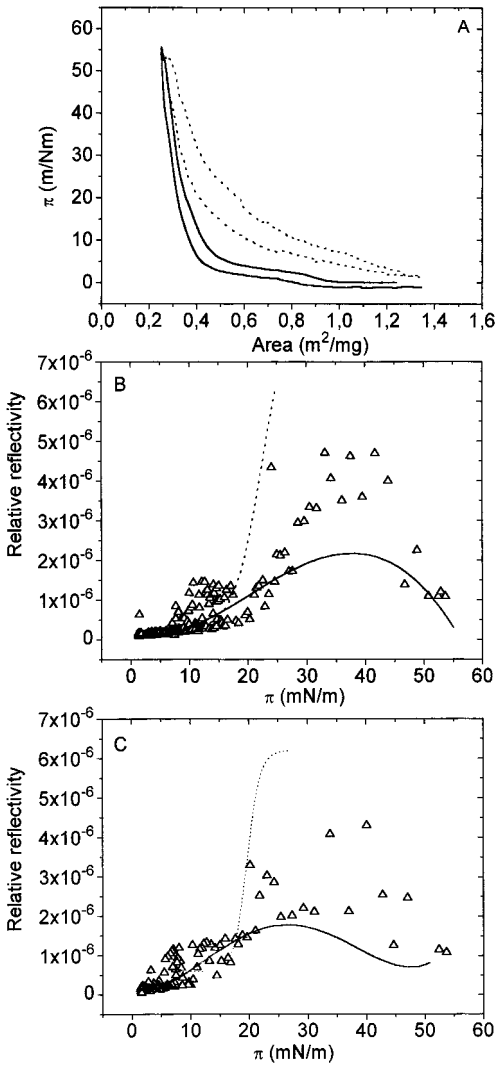

Figure 9. (A) $\pi-A$ isotherms for monopalmitin−β-casein mixed monolayers at pH 5 (—) and pH 7 (···). (B and C) Relative reflectivity as a function of surface pressure during the compression and expansion, respectively, for monopalmitin−β-casein monolayers at pH 7 (Δ) and at a shutter speed of 1:250 s. Temperature 20 °C. Monopalmitin mass fraction in the mixture: $X = 0.8$. The line fit for monopalmitin (—) and β-casein (···) pure monolayers are included in plots B and C.

monopalmitin and β-casein could exist, β-casein molecules adopting different structures in the anisotropic liquid-condensed monopalmitin monolayer depending on the pH and the surface pressure, as described above. However, at surface pressures higher than that for β-casein collapse, the mixed monolayers were practically dominated by monopalmitin molecules. That is, at higher surface pressures, collapsed β-casein residues could be displaced from the interface by monopalmitin molecules. A similar phenomenon was deduced for β-casein−monoolein mixed monolayers (Rodríguez Patino et al., 1999d).

The $I-\pi$ plots for monolayer compression (Figure 7B) and expansion (Figure 7C) followed essentially the same trends as those for a mixture with a mass fraction of monopalmitin of 0.2, discussed above. Briefly, at $\pi <$ 20 mN/m, the $I-\pi$ plots for compression and expansion (Figure 7B,C, respectively) were the same as those for pure components. In this region a liquid-condensed domain of monopalmitin existed in the ambient homogeneous phase of liquid-expanded monopalmitin and β-casein, during the compression (Figure 8A), and typical 2D foams, during the expansion (Figure 8D). The main difference was observed in the region near the β-casein collapse ($20 < \pi < 30$ mN/m), because the relative reflectivity of the mixed film was lower than that for pure β-casein. This suggests that as the content of monopalmitin in the mixture increases, β-casein residues are more easily displaced from the interface toward a sublayer beneath the monopalmitin monolayer. Figure 8B shows a characteristic squeezing out phenomenon. In fact, many liquid-condensed domains of monopalmitin—the dark domains are due to monopalmitin with a liquid-condensed structure, as confirmed by turning the analyzer from 60° to 120° (data not shown)—are floating over a sublayer of collapsed β-casein molecules—characterized by a completely white image.

Figure 8C shows the frontier between a region of collapsed β-casein molecules and closely packed liquid-condensed domains of monopalmitin near its collapse ($\pi = 43$ mN/m). The existence of these isolated spots with collapsed β-casein residues is the cause of the peaks observed in the $I-\pi$ plot (Figure 7B). It is possible that, as a consequence of the high monolayer compression near the monopalmitin collapse, some degree of mixing between monopalmitin molecules and β-casein residues could take place, especially during the expansion (Figure 7C).

Monopalmitin−β-Casein Mixed Film at a Mass Fraction of Monopalmitin in the Mixture of 0.8. In Figure 9 we show the $\pi-A$ isotherm for a compression−expansion cycle (Figure 9A) and the $I-\pi$ plot for compression (Figure 9B) and expansion (Figure 9C) of monopalmitin−β-casein mixed monolayer at 0.8 in mass fraction of monopalmitin in the mixture. In Figure 10 we show the BAM images for mixed films at some representative surface pressures during the compression−expansion cycle.

The behavior of β-casein−monopalmitin mixed films at $X = 0.8$ was different from those for lower concentrations of monopalmitin in the mixture (Figures 5−8), as deduced from $\pi-A$ isotherms (Figure 9A), $I-\pi$ plots (Figure 9B,C), and BAM images (Figure 10). During the compression and expansion at $\pi < 20$ mN/m, the $I-\pi$ plots followed the same trends as the pure components but with a higher number of peaks with a higher intensity. The BAM images (Figure 10A,B) suggest that these results are due mainly to a practically single monopalmitin monolayer. In fact, as for monopalmitin monolayers (Figure 2), liquid-condensed domains (Figure 10A) from the homogeneous ambient phase with a liquid-expanded structure, which derived from initial dentritic-shaped domains at the lower π (not shown), were observed. These typical dentritic-shaped domains of monopalmitin (Rodríguez Patino et al., 1999b) were not observed at the lower concentrations of monopalmitin in the mixture. The liquid-condensed domains grew in size, and the monolayer was covered with liquid-condensed domains as the surface pressure was increased. Thus, at higher surface pressures, liquid-condensed domains of monopalmitin (Figure 10B) dominated the mixed monolayer. Each domain did not have a uniform intensity, and this intensity changed with the analyzer angle (data not shown), which suggests that monopalmitin molecules dominated the composition of the monolayer in this region.

The only difference compared with monopalmitin was observed during the monolayer expansion. The 2D foam

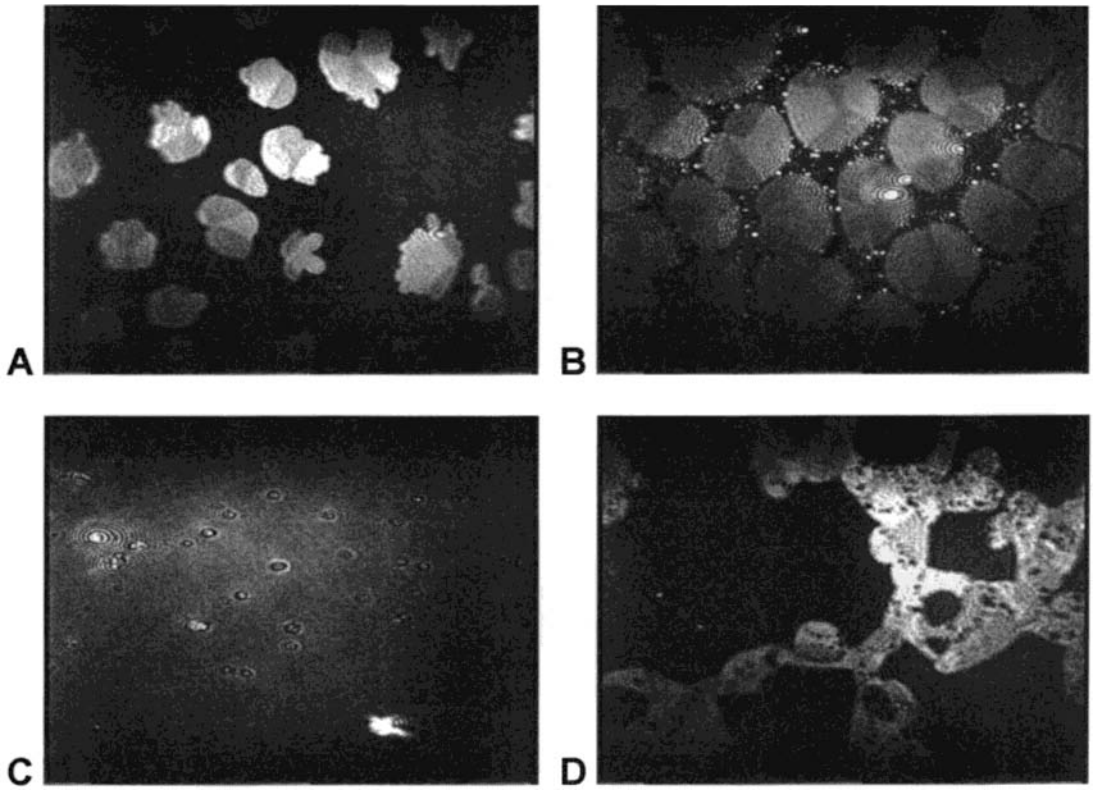

Figure 10. Visualization of monopalmitin-β-casein mixed monolayers by Brewster angle microscopy at 20 °C and pH 7. (A) $\pi =$ 10 mN/m, (B) $\pi = 20$ mN/m (near the β-casein collapse), (C) $\pi = 53$ mN/m (at the monopalmitin collapse), and (D) 2D foam after monolayer expansion at $\pi = 6$ mN/m. Monopalmitin mass fraction in the mixture: $X = 0.8$. The horizontal direction of the image corresponds to 630 μm and the vertical direction to 470 μm.

for the mixed monolayer (Figure 10D) consisted of collapsed plateau borders with foam cells containing mainly a liquid-condensed monolayer at higher surface pressures and finally with liquid-condensed/liquid-expanded structures and probably β-casein homogeneous residues at the maximum area, as the surface pressure approaches zero. However, the shape of the 2D foam is different from that of monopalmitin monolayer (Rodríguez Patino et al., 1999b). This suggests the existence of some degree of mixing in the plateau borders between monopalmitin and closely packed β-casein residues, which produced peaks with an intensity for the mixed film higher than that for the pure components.

The prevalence of monopalmitin in the mixture is especially evident in the region of higher surface pressures ($\pi > 25$ mN/m) after the β-casein collapse. During the monolayer compression the $I-\pi$ plot (Figure 9B) followed the same trends as for monopalmitin with the absence of peaks with high intensity, characteristic of β-casein collapsed phase (the camera was not saturated during the monolayer compression). The BAM images corroborated the absence of β-casein collapsed domains in this region. However, we cannot conclude that the protein is completely displaced from the interfacial region because the peak intensity was higher than that for monopalmitin, which suggests that some degree of mixing exists as the mixed film is compressed at higher surface pressures. Finally, the relative intensity decreased as the surface pressure was close to that for monopalmitin collapse (Figure 9B). The monolayer-collapsed phase at ca. 53.4 mN/m was characterized by a homogeneous morphology (Figure 10C).

During the monolayer expansion, in the region of $20 < \pi < 53$ mN/m, the $I-\pi$ plot passed between those for pure components but without any peak with an intensity characteristic of β-casein. This result suggests that even at higher surface pressures, with a high content of monopalmitin in the mixture, some interaction between components in the mixed films exist. As a consequence of these interactions, the β-casein residues displaced by monopalmitin molecules toward the sublayer region during the compression return to the interface with the monolayer expansion. This hypothesis is in agreement with the 2D foam morphology at the lower surface pressures (Figure 10D) and with the reproducibility of the $\pi-A$ isotherms after a waiting time at the maximum area.

Effect of pH on β-Casein−Monopalmitin Mixed Films. For single-component monolayers, the effect of pH on monolayer structure is different for monopalmitin than for β-casein (Figures 1 and 3). The monopalmitin monolayer structure is practically independent of the aqueous-phase pH (data not shown). However, the structure of β-casein monolayers is more condensed in acidic subphases (Figure 3A). Given that β-casein has an isoelectric point of about 4.9−5.2 in water, condensation of the monolayer structure observed with β-casein films on acidic aqueous subphase must be attributed to a reduction in the repulsive interactions between negative amino acid residues. This is due to the fact that at pH 5 the overall charge of β-casein molecules approaches zero (Atkinson et al., 1997; Dickinson et al., 1993; Gau et al., 1994; Rodríguez Niño et al., 1998c). For β-casein−monopalmitin mixed films, the monolayer structure is more condensed and the hysteresis in the $\pi-A$ isotherm during the compression−expansion cycle is higher on acidic subphases, which is an indication of the influence of the protein in the mixed film (Figures 5A, 7A, and 9A). However, from the BAM images, at a

microscopic level, it is impossible to observe significant differences in morphology and relative intensity as a function of the aqueous-phase pH. Due to the fact that food emulsions and foams are often submitted to pH variations in manufacturing and even during their storage (Dickinson, 1992), the effect of pH on the structural characteristics and morphology of protein−lipid mixed films needs deeper study including other lipids, phospholipids, and proteins. This study, including higher pH variations, is under way at present.

CONCLUSIONS

The surface pressure−area isotherms and BAM images of monopalmitin−β-casein mixed films spread on buffered water at pH 5 and 7 and at 20 °C indicate that the structural characteristics and morphology of these mixed films are very dependent on the surface pressure and monolayer composition. The evolution with the surface pressure of the relative reflectivity of BAM images gives complementary information on the interactions and structural characteristics of spread mixed films deduced from $\pi-A$ isotherms. These results have shown that for β-casein−monopalmitin mixed films, the distribution of components at the interface is not uniform on a microscopic scale but heterogeneous. At higher surface pressures, after the β-casein collapse, a characteristic squeezing out phenomena was observed with liquid-condensed domains of monopalmitin floating over a sublayer of collapsed residues of β-casein. The relative reflectivity makes possible determination of the relative thickness of the monolayer (in accordance with eq 1), as for single components (Rodríguez Patino et al., 1999b,c). It can be deduced that the relative thickness of the mixed film increases with the surface pressure and tends to a maximum at the region close the β-casein collapse and then decreases with surface pressure to lower values characteristic for monopalmitin monolayers. Over the overall range of existence of the mixed film, the monolayer presents some heterogeneity due to the fact that liquid-condensed domains of monopalmitin and islands of collapsed β-casein residues are present during the monolayer compression−expansion cycle, giving noise peaks with high relative film thickness. At the monopalmitin monolayer collapse, the mixed film is practically dominated by the presence of monopalmitin. The prevalence of monopalmitin increases with the amount of monopalmitin in the mixture and at higher surface pressures. However, some degree of interactions exist between monopalmitin and β-casein in the mixed film, which are more pronounced as the monolayer is compressed at the highest surface pressures. The consequences of these interactions are more evident during the monolayer expansion, with the formation of 2D foams.

Displacement of the milk proteins β-casein, β-lactoglobulin, and α-lactoglobulin from the air−water interface by the nonionic surfactant Tween 20 has been observed recently by imaging Langmuir−Blodgett films using an atomic force microscope (Mackie et al., 1999; Gunning et al., 1999). In these studies the protein displacement was attributed to a novel "orogenic" mechanism. The orogenic displacement mechanism can explain the effects observed in this work at a higher scale, as a function of surface pressure.

In summary, on a microscopic level the distribution of monopalmitin and β-casein in mixed spread films at the air−water interface depends on the surface pressure and the lipid−protein ratio in the mixed film. From a practical point of view, these results suggest that in real food emulsions and foams containing lipids and proteins as emulsifiers, the emulsion droplets and foam bubbles may have a different interfacial composition with repercussions on their stability.

ACKNOWLEDGMENT

We thank Prof. D. Horne for providing the β-casein sample and Danisco Ingredients for providing the monopalmitin sample.

LITERATURE CITED

Atkinson, P. J.; Dickinson, E.; Horne, D. S.; Richardson, R. M. Neutron Reflectivity of adsorbed β-casein and β-lactoglobulin at the air/water interface. *J. Chem. Soc., Faraday Trans.* **1995**, *1*, 2847−2854.

Atkinson, P. J.; Dickinson, E.; Horne, D. S.; Leaver, J.; Leermakers, F. A. M.; Richardson, R. M. β-Casein adsorbed layer structures predicted by self-consistent-field modeling: comparison with experiment. In *Food Colloids: Proteins, Lipids and Polysaccharides*; Dickinson, E., Bergesntahl, B., Eds.; Royal Society of Chemistry: Cambridge, 1997; pp 217−228.

Azzam, R. M. A.; Bashara, N. M. *Ellipsometry and Polarized Light*; North-Holland: Amsterdam, 1992.

Bos, M.; Nylander, T.; Arnebrant, T.; Clark, D. C. Protein/emulsifier interactions. In *Food Emulsions and their Applications*; Hasenhuette, G. L., Hartel, R. W., Eds.; Chapman & Hall: New York, 1997; pp 95−146.

Cayot, P.; Lorient, D. Structure−Function Relationships of Whey Proteins. Food Proteins and their Applications. In *Emulsions and Emulsion Stability*; Damodaran, S., Paraf, A., Eds.; Marcel Dekker: New York, 1997; pp 225−256.

Dalgleish, D. Food Emulsions. In *Emulsions and Emulsion Stability*; Sjöblom, J., Ed.; Marcel Dekker: New York, 1996; pp 287−325.

Dalgleish, D. G. Structure−Function relationships of caseins. In *Food Proteins and their Applications*; Damodaran, S., Paraf, A., Eds.; Marcel Dekker: New York, 1997; pp 199−223.

Food Proteins and their Applications; Damodaran, S., Paraf, A., Eds.; Marcel Dekker: New York, 1997.

de Mul, M. N. G.; Mann, J. A., Jr. Determination of the thickness and optical properties of a Langmuir film from the domain morphology by Brewster angle microscopy. *Langmuir* **1998**, *14*, 2455−2466.

Dickinson E. *An Introduction to Food Colloids*; Oxford University Press: Oxford, 1992.

Dickinson, E.; Horne, D. S.; Phipps, J. S.; Richardson, R. M. A neutron reflectivity study of the adsorption of β-casein at fluid interface. *Langmuir* **1993**, *9*, 242−248.

Food Emulsions; Friberg, S. E., Larsson, K., Eds.; Marcel Dekker: New York, 1997.

Gau, C. S.; Yu, H.; Zografi, G. Surface viscoelasticity of β-casein monolayers at the air/water interface by electrocapillary wave diffraction. *J. Colloid Interface Sci.* **1994**, *162*, 214−221.

Gunning, A. P.; Mackie, A. R.; Wilde, P. J.; Morris, V. J. *In situ* observation of the surfactant-induced displacement of proteins from a graphite surface by atomic force microscopy. *Langmuir* **1999**, *15*, 4636−4640.

Mackie, A. R.; Gunning, A. P.; Wilde, P. J.; Morris, V. J. Orogenic displacement of protein from the air/water interface by competitive adsorption. *J. Colloid Interface Sci.* **1999**, *210*, 157−166.

Nylander, T.; Ericsson, B. Interactions between proteins and polar lipids. In *Food Emulsions*; Friberg, S. E., Larsson, K., Eds.; Marcel Dekker: New York, 1997; pp 189−233.

Rodríguez Niño, M. R.; Carrera, C. S.; Rodríguez Patino, J. M. Interfacial characteristics of β-casein spread films at the air−water interface. *Colloids Surfaces B* **1998c**, *12*, 161−173.

Rodríguez Niño, M. R.; Rodríguez Patino, J. M. Surface tension of protein and insoluble lipids at the air-aqueous phase interface. *J. Am. Oil Chem. Soc.* **1998a**, *75*, 1233−1239.

Rodríguez Niño, M. R.; Rodríguez Patino, J. M. Surface tension of bovine serum albumin and Tween 20 at the air-aqueous phase interface. *J. Am. Oil Chem. Soc.* **1998b**, *75*, 1241−1247.

Rodríguez Niño, M. R.; Wilde, P. J.; Clark, D. C.; A.; Rodríguez Patino, J. M. Rheokinetic analysis of protein films at the air-aqueous phase interface. 2. Bovine serum albumin adsorption from sucrose aqueous solutions. *J. Agric. Food Chem.* **1997b**, *45*, 3016−3021.

Rodríguez Niño, M. R.; Wilde, P. J.; Clark, D. C.; Husband, F. A.; Rodríguez Patino, J. M. Rheokinetic analysis of protein films at the air-aqueous phase interface. 1. Bovine serum albumin adsorption on ethanol aqueous solutions. *J. Agric. Food Chem.* **1997a**, *45*, 3010−3015.

Rodríguez Niño, M. R.; Wilde, P. J.; Clark, D. C.; Husband, F. A.; Rodríguez Patino, J. M. Rheokinetic analysis of bovine serum albumin and Tween 20 mixed films on aqueous solutions. *J. Agric. Food Chem.* **1998a**, *46*, 2177−2184.

Rodríguez Niño, M. R.; Wilde, P. J.; Clark, D. C.; Rodríguez Patino, J. M. Surface dilational properties of protein and lipids films at the air−water interface. *Langmuir* **1998b**, *14*, 2160−2166.

Rodríguez Patino, J. M.; Rodríguez Niño, M. R.; Carrera, C. S. Adsorption of whey protein isolates at the oil−water interface as a function of processing conditions. A rheokinetic study. *J. Agric. Food Chem.* **1999a**, *47*, 2241−2248.

Rodríguez Patino, J. M.; Carrera, C. S.; Rodríguez Niño, M. R. Morphological and structural characteristics of monoglyceride monolayers at the air−water interface observed by Brewster angle microscopy. *Langmuir* **1999b**, *15*, 2484−2492.

Rodríguez Patino, J. M.; Carrera, C. S.; Rodríguez Niño, M. R. Structural and morphological characteristics of β-casein monolayers at the air−water interface. *Food Hydrocolloids* **1999c**, *13*, 401−408.

Rodríguez Patino, J. M.; Carrera, C. S.; Rodríguez Niño, M. R. Is Brewster angle microscopy a useful technique to distinguish between isotropic domains in β-casein-monoolein mixed monolayers at the air−water interface? *Langmuir* **1999d**, *15*, 4777−4788.

Rodríguez Patino, J. M.; Ruíz, M.; de la Fuente, J. Monostearin monolayers spread on aqueous solutions containing ethanol. *J. Colloid Interface Sci.*, **1992**, *154*, 146−159.

Rodríguez Patino, J. M.; Ruíz, M.; de la Fuente, J. The effect of sugars on monostearin monolayers. *J. Colloid Interface Sci.* **1993**, *157*, 343−354.

Sjöblom, J. *Emulsions and Emulsion Stability*; Marcel Dekker: New York, 1996.

Received for review March 8, 1999. Revised manuscript received August 31, 1999. Accepted September 21, 1999. This research was supported by the European Community through Grant FAIR-CT96-1216 and by CICYT through Grant ALI97-1274-CE.

JF9902696